IOPscience iopscience.iop.org

Home Search Collections Journals About Contact us My IOPscience

A polarization-independent and low scattering transmission grating for a distributed feedback cavity based on holographic polymer dispersed liquid crystal

This article has been downloaded from IOPscience. Please scroll down to see the full text article.

2011 J. Opt. 13 085501

(http://iopscience.iop.org/2040-8986/13/8/085501)

View the table of contents for this issue, or go to the journal homepage for more

Download details:
IP Address: 159.226.165.151
The article was downloaded on 06/09/2012 at 02:48

Please note that terms and conditions apply.

IOP Publishing Journal of Optics
J. Opt. **13** (2011) 085501 (7pp) doi:10.1088/2040-8978/13/8/085501

A polarization-independent and low scattering transmission grating for a distributed feedback cavity based on holographic polymer dispersed liquid crystal

Wenbin Huang[1,2], Shupeng Deng[1,2], Wencui Li[1,2], Zenghui Peng[1], Yonggang Liu[1], Lifa Hu[1] and Li Xuan[1]

[1] State Key Laboratory of Applied Optics, Changchun Institute of Optics, Fine Mechanics and Physics, Chinese Academy of Science, Changchun 130033, People's Republic of China
[2] Graduate School of Chinese Academy of Science, Beijing 100039, People's Republic of China

E-mail: wbhuang1987@gmail.com

Received 27 April 2011, accepted for publication 5 July 2011
Published 28 July 2011
Online at stacks.iop.org/JOpt/13/085501

Abstract
By using acrylate monomers and increasing the fabricating temperature to the nematic–isotropic transition point of liquid crystal, a polarization-independent holographic polymer dispersed liquid crystal (HPDLC) transmission grating is demonstrated, which is different from the conventional anisotropic grating forms at room temperature. Also, about 25% more liquid crystal is phase separated out to form the pure liquid crystal layer and the scattering loss of the Bragg diffraction grating is reduced from 8% to 4%. These results are explained by means of optical measurements. The randomly aligned liquid crystal (LC) molecules in the pure LC layer of the transmission grating bring in a much higher refractive index contrast for photons of specific frequency propagating along the grating vector, which results in a much more effective light feedback effect. Experimental results of this transmission grating as a distributed feedback laser show a lasing output with a full width at half maximum (FWHM) of about only 0.6 nm and a threshold of 6 μJ/pulse.

Keywords: holographic polymer dispersed liquid crystal, volume transmission gratings, distributed feedback laser

(Some figures in this article are in colour only in the electronic version)

1. Introduction

Holographic polymer dispersed liquid crystal (HPDLC) gratings are formed by polymerization-induced anisotropic phase separation of liquid crystal from the polymer matrix. In this method, coherent laser beams are used to irradiate onto a homogeneous syrup containing mainly photoinitiator, monomers and liquid crystal. Monomers in the bright interference fringes undergo a fast free-radical photopolymerization, then counter-diffusions of liquid crystal and monomers are initialized due to the resulting concentration gradient. A miscibility gap is thus reached and the liquid crystal phase separates out from monomers in the dark fringes. Finally a stratified composite of alternating layers corresponding to interference fringe patters of liquid crystal and polymers is formed [1]. This nanostructure fabricated by a holographic technique brings in refractive index modulation at periodicities comparable to the optical wavelength, which

 © 2011 IOP Publishing Ltd Printed in the UK & the USA

endows HPDLC structures with the ability to modulate light [2]. Moreover, due to the liquid crystal inherent nature of an anisotropic dielectric, it can be aligned in the direction of the applied electric field and the refractive contrast of HPDLC can be modified continuously. In the past several years HPDLC has drawn a great deal of research attention and has been exploited in applications in fields such as reflective flat panel displays [3], optical switches for telecommunications [4], switchable optical phase modulators [5], and switchable focus lenses [6].

More recently, special attention has been given to laser emission from dye-doped HPDLC structures. Jakubiak *et al* demonstrated lasing from the dye-doped reflection gratings [7]. Laser action from dye-doped HPDLC transmission was also observed by Hsiao [8] and Liu [9]. A better lasing emission performance with low threshold and narrow linewidth has been reported in two-dimensional (2D) HPDLC square-lattice structures [10]. Although the transmission grating has the advantage of a much longer gain length compared with the reflection grating, there are still two drawbacks influencing the lasing performance of a dye-doped transmission grating. Firstly, liquid crystal molecules in the LC layer of the transmission grating have a preferred orientation along the grating vector, then for feedback lights propagating along the grating vector, the refractive index (RI) modulation is as low as 10^{-5} [8], and effective light feedback which is essential for lasing output is thus difficult to obtain. This self-alignment of LC molecules in the transmission grating is implied by the strong dependence of optical properties on the polarization state of incident light, which has been fully explored by Vardanyan's polymer scaffolding model [11] and Butler's calculation [12] based on the anisotropic coupled wave theory. Secondly, huge scattering loss due to the appearance of wavelengths comparable with the liquid crystal droplet size is also a remarkable restriction on the application of HPDLC transmission grating microlasers.

Caputo's team demonstrated [13] in their materials system (mainly an ultraviolet (UV) curable Norland optical adhesive (NOA) system) that they could prevent the growth of nematic liquid crystal (NLC) droplets by recording the HPDLC transmission grating above the LC clearing point, known as POLICRYS, while the orientation of liquid crystal along the grating vector in POLICRYS remains [5]. In this work, we present a polarization-independent and low scattering transmission grating for a distributed feedback (DFB) laser cavity by using acrylate monomers and increasing the fabricating temperature to the liquid crystal clearing point. Lasing performance of this dye-doped transmission grating is also presented which shows a narrow full width at half maximum (FWHM) of about 0.6 nm and a low threshold of 6 μJ/pulse.

2. Experimental part

2.1. Materials

In our experiments, to control the effective functionality of the monomers, two kinds of acrylate monomers are selected, one is difunctional phthalic diglycol diacrylate

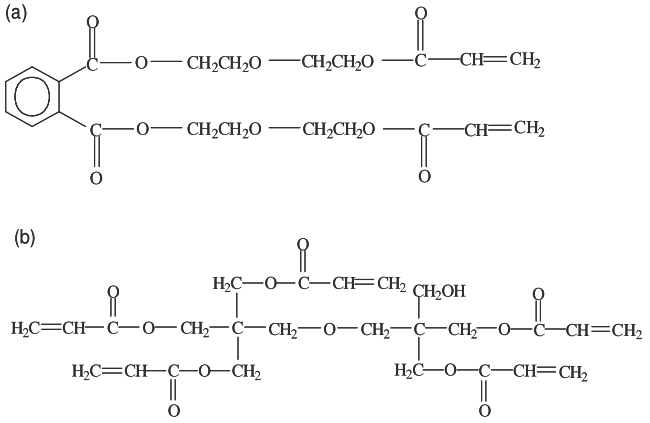

Figure 1. Chemical structures of PDDA (a) and DPHPA (b).

(PDDA) (Eastern Acrylic Chem. Tech. Co., Ltd, Beijing, n_D = 1.4977 at 20 °C), the other is penta-functional dipentaerythritol hydroxyl pentaacrylate (DPHPA) (supported by Aldrich, n_D = 1.49 at 20 °C). The chemical structures of PDDA and DPHPA are shown in figures 1(a) and (b) respectively. *N*-vinylpyrrolidone (NVP) which serves as a solvent and cross-linker (supported by Aldrich, n_D = 1.512 at 20 °C), nematic liquid crystal TEB30A (Slichem Co., Ltd, Shi Jia Chuang, China, Δn = 0.1703, n_e = 1.6925 at 20 °C), photoinitiator rose Bengal (supported by Aldrich), and coinitiator *N*-phenylglycine (supported by Aldrich) are also added. The lasing dye, 4-dicyanomethylene-2-methyl-6-p-dimethylaminostyryl-4H-pyan (DCM) (from Sigma-Aldrich) is dissolved in the mixture as an active medium, These ingredients were mixed together with weight ratios of 30.1%, 30.2%, 9.1%, 27.4%, 0.45%, 1.8%, and 1%, respectively; then they were stirred for 12 h in the dark until a homogeneous and viscous mixture was obtained. Finally a droplet of the mixture was sandwiched by capillarity between two sealed glass plates separated by Mylar spacers with a diameter of 12 μm.

2.2. Determination of the refractive index of pure polymer

A monomer mixture composed of DPHPA, PDDA, and NVP with weight ratios the same as the HPDLC sample was obtained. After being mechanically blended to form a homogeneous mixture, the monomer mixture was carefully wiped on the polishing prism of the Abbe Refractometer (Shanghai Optical Instrument Import & Export Co., Ltd). Then it was irradiated under UV light for about an hour to initiate photo-induced polymerization of the monomers and a pure polymer membrane was formed on the surface of the testing prism. The measured value of pure polymer refractive index under visible light is 1.5252, very close to n_o (1.522) of liquid crystal.

2.3. Experimental setup for fabrication

The experimental setup for the fabrication of the transmission grating is shown in figure 2. The sample was mounted on a heating stage with a thermocouple embedded in it for temperature measurement. The fabrication temperature

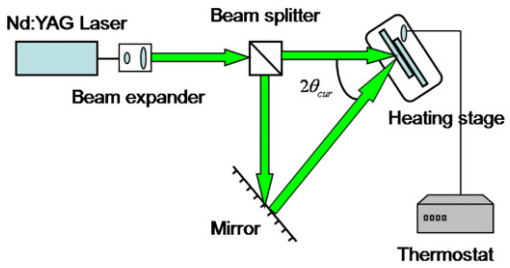

Figure 2. Schematic setup for the preparation of transmission gratings: $2\theta_{cur}$—total curing angle.

was then kept constant ranging from 20 to 62 °C by the thermostat with an accuracy of 0.1 °C, where T_C (61 °C) is the nematic–isotropic phase transition temperature of the LC. Two interfering laser beams, from a 532 nm Nd:YAG laser, impinged on the sample symmetrically to the normal of the glass cell with an interference angle of $\theta_{cur} = 20°$. The corresponding grating pitch is 777 nm derived by $\Lambda = \frac{\lambda_{532}}{2\sin\theta_{cur}}$ and the Q factor of the grating under a He–Ne probing beam is 55. The intensity of each recording beam was 3.75 mW cm^{-2} and the exposure time was around 3 min. Finally, the cell was exposed in daylight for about two days so that monomers in the regions outside the grating were polymerized and the grating was optically stable. The absorbance and photoluminescence (PL) of doped DCM were almost unchanged after the grating writing and daylight post-curing process, indicating good photostability of the lasing dye. For the scanning electron microscopy (SEM) test, the samples were soaked in alcohol for about 12 h to remove LC from the gratings, and then gold nanoparticles were sputtered onto the surface of the samples.

The diffractive properties of samples were characterized by a low power (1 mW) He–Ne laser at room temperature, the s or p polarization state was obtained by rotating a polarizer in front of the He–Ne laser. And its incident angle was adjusted to satisfy the Bragg condition $\sin\theta_B = \lambda_{633}/2\bar{n}\Lambda$ ($\bar{n}$ stands for average refractive index of the grating, Λ is the grating pitch). We measured the intensity: I_{in} the incident laser intensity; I_1 the first-order diffraction beam intensity by the Bragg grating; I_0 the zero-order diffraction beam intensity; I_{re} the intensity of light reflected by the glass cell.

2.4. Lasing measurement

A Q-switched frequency-doubled Nd:YAG pulsed laser operating at 532 nm with a pulse duration of 8 ns and repetition rate of 8 Hz was used as the pumping source for the lasing measurement, the energy from the laser was measured by a pulse energy meter. The schematic setup of the lasing measurement is shown in figure 3. A cylindrical lens with a focal length of 30 cm was used to shape the pump beam into a narrow strip gain area of ~10 mm length and 0.1 mm width along the grating vector, this pumping strip could cover thousands of periods of the grating, and ensures effective distributed feedback. A fiber pigtail detector was placed facing the lasing output to collect the signal, which was coupled to a spectrometer (with a resolution of ~0.25 nm).

The absorption and photoluminescence spectra of the DCM-doped HPDLC film could be found elsewhere [9]; considering the reabsorption of the dye, the lasing action could be expected in the range of 590–750 nm.

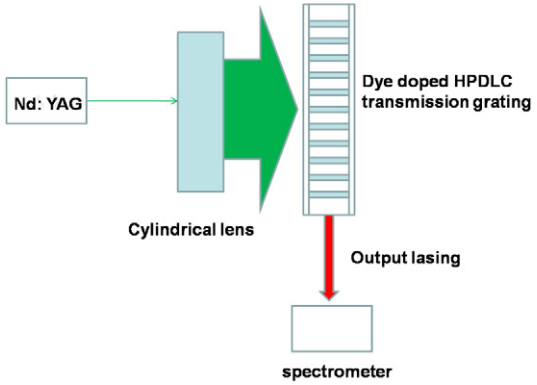

Figure 3. Schematic setup for the lasing measurement.

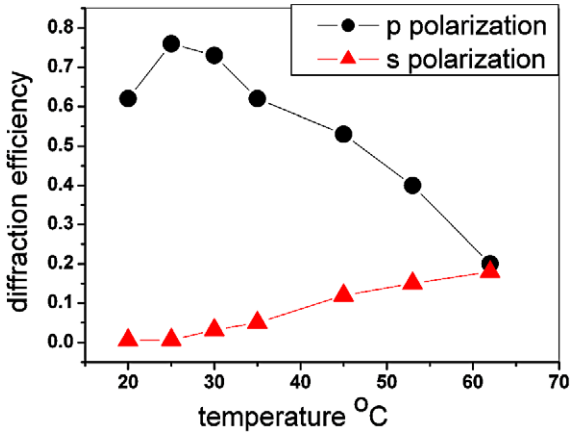

Figure 4. Grating diffraction efficiency measured for p (circular) and s (triangle) waves as a function of fabricating temperature. The readout temperature was 25 °C.

3. Results and discussion

3.1. Polarization-independent transmission grating

The diffraction efficiency of the transmission grating is defined as the ratio of the intensity of the first-order diffracted beam to that of the incident beam subtracting the reflection by the surface of glass cell, $\eta = I_1/(I_{in} - I_{re})$. The dependence of grating diffraction efficiency measured for p and s polarization on the recording temperature is shown in figure 4. The reading temperature was 25 °C. It can be seen that η_p reaches a maximum (76%) at 25 °C and then decreases to around 20% by 62 °C, this shows that for conventional HPDLC gratings making use of p polarization, the optimum fabricating temperature is 25 °C. While η_s increases steadily from a negligible value (1%) to around 20% accompanying the increased fabricated temperature. At a first glance of these two results, one cannot tell whether the abrupt decrease of η_p and contrasting increase of η_s with the increasing recording temperature are the result of a bad phase separation of the transmission grating or of the alternation of LC molecule

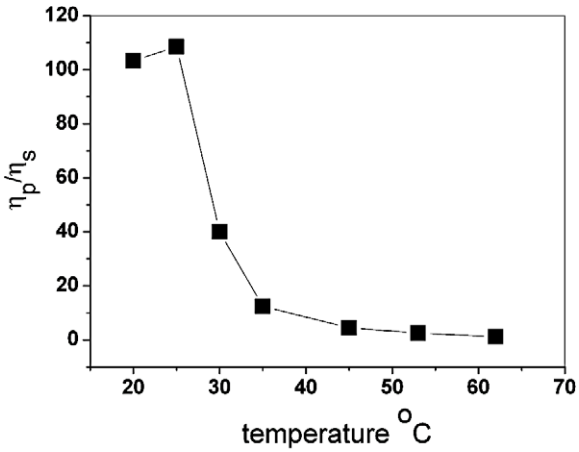

Figure 5. Diffraction efficiency ratio for p and s waves as a function of recording temperature.

alignment or of a combination of these two reasons, and they will be checked next.

It is well known in HPDLC transmission gratings that the difference between the diffraction efficiency for p-polarized light and that for s-polarized light carries the message about liquid crystal alignment in the pure LC layer [14, 21], and we utilized the diffraction efficiency ratio for p and s waves as a grating anisotropic parameter to quantify the anisotropy of the grating, The grating anisotropy parameter as a function of fabricating temperature is shown in figure 5. The huge anisotropic parameter of the room temperature fabricated grating verifies the fact that in conventional gratings liquid crystal molecules are aligned perpendicular to the HPDLC planes. As the fabrication temperature increases, the anisotropy parameter goes down and reaches a value of about 1 by 62 °C, which shows that the highly anisotropic gratings become optically isotropic and the liquid crystal molecules in the pure LC layer are randomly aligned. The following discussions are based on the comparison between 25 °C (room temperature) fabricated anisotropic grating and 62 °C (high temperature) fabricated isotropic grating.

It is worth mentioning that the high temperature fabricated counterpart POLYCRIPS are typically highly anisotropic with the uniform alignment of the LC director along the grating vector. The difference with POLYCRIPS may come from different reaction mechanisms between thiol-ene polymer and acrylate polymer. The monomer used in POLYCRIPS is UV curable thiol-ene adhesive from Norland Inc. Due to the late gelation in the thiol-ene system, most of the double bonds are consumed while the precursors are still in the liquid crystal state [15]. The resulting polymer is elastic and smooth. Polymer filaments are not present in such a system and this can be found out using POLYCRIPS, which is contrary to conventional chain-growth reactions of acrylic monomers, where gelation appears early in the reaction (<5% conversion). Once the gel is established, further conversion of double bonds may exist in the form of polymer filaments which smear the regularity of the interface, which can been seen from our SEM pictures shown in figure 6. Considering the narrow width of the pure LC layer (around 100 nm) in our samples, there may be some polymer network existing in the pure LC layer. Polymer networks or polymer filaments have been demonstrated in LC modulator applications to be effective ways to stabilize or align LC molecules [16]. Finally, we arrive at our explanation that the polymer network or polymer filaments residing in the pure LC layer could 'freeze' and 'reserve' the LC original state during the curing process. Thus, our high temperature fabricated grating is isotropic at room temperature.

3.2. Calculation for the phase separation

According to the SEM analysis in figure 6, the LC rich region in our samples is devoid of any specific liquid crystal droplets and resembles the scaffolding morphology [11], so the calculation below does not need to incorporate assumptions concerning the shape and size distribution of LC droplets or LC molecule alignment inside the droplet. These assumptions are strongly required in droplet morphology to explain the diffractive properties [14, 17, 22]. A simple and reasonable model for grating structure is thus proposed (shown in figure 7) whereby the composite transmission grating is composed of two regions with the same width of half the grating pitch. One is a low refractive index region formed by pure polymer with some randomly aligned LC molecules trapped in it. The index of this region can be expressed as:

$$n_a = n_{p(LC)} = cn_{iso} + (1 - c)n_p, \tag{1}$$

where c is the volume concentration of liquid crystal in the low index region, n_p is the refractive index of pure polymer, whose experimental value is 1.5252, and $n_{iso} = \sqrt{\frac{2}{3}n_0^2 + \frac{1}{3}n_e^2} = 1.582$ is the refractive index of liquid crystal in the isotropic state. The other is a high refractive region formed by a solid polymer matrix and a pure liquid crystal layer. The refractive index of this region is:

$$n_b = fn_{LC} + (1 - f)n_{p(LC)}, \tag{2}$$

where f is the filling fraction of liquid crystal in the high refractive index region, $n_{p(LC)}$ is the refractive index of the polymer matrix, and n_{LC} is the refractive index of the pure LC layer, which is dependent on the alignment of LC molecules and the polarization state of the incident probe beam. The parameters c and f contain all the information about the liquid crystal distribution across the transmission grating. For the isotropic gratings fabricated at high temperature, the value of n_{LC} equals that of n_{iso} and the refractive index modulation (n_1) can be calculated by Kogelnik's isotropic coupled wave theory [18]:

$$(n_b - n_a)/2 = n_1 = \frac{\arcsin\sqrt{\eta_s}\lambda_{633}\cos\theta_B}{\pi L} \tag{3}$$

θ_B is the Bragg angle within the material. $n_1 = 0.0072$ was determined at $\eta_s = 18.6\%$. Combining the average refractive index of the transmission grating:

$$(n_a + n_b)/2 = n_o = 0.72n_{p(pure)} + 0.28n_{iso} = 1.541. \tag{4}$$

We finally arrived at $c_{62\,°C} = 0.151$, $f_{62\,°C} = 0.298$, and the width of the pure LC layer is approximately 116 nm, which

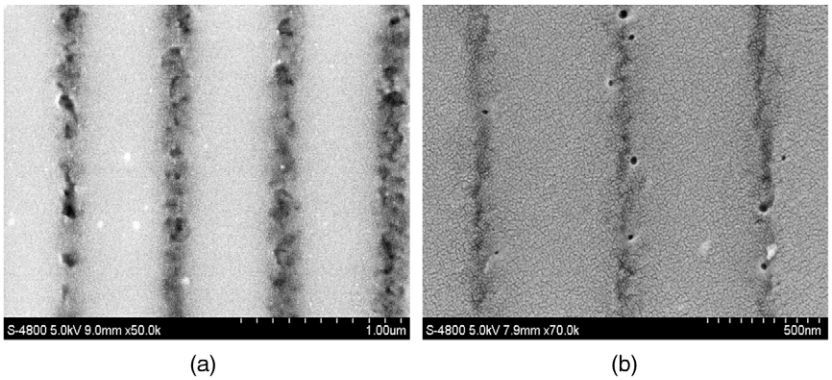

Figure 6. SEM pictures of (a) a high temperature fabricated grating (b) a room temperature fabricated grating.

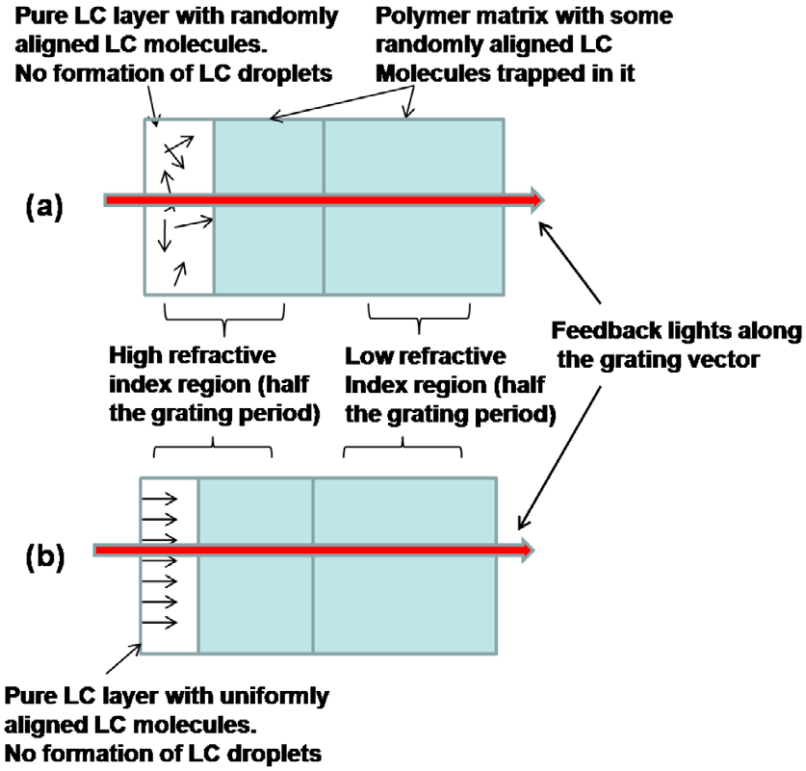

Figure 7. Schematic illustration for one period of (a) high temperature fabricated grating, (b) room temperature fabricated grating.

is consistent with the SEM analysis. The refractive index difference between the liquid crystal rich and polymer rich for feedback lights along the grating is 0.0144 (derived from $\Delta n = n_b - n_a$).

For the grating fabricated at room temperature, we measured its diffraction efficiency at a temperature of 62 °C; the above calculation can be used under this condition as the grating above the clearing point exhibits characteristics of an isotropic grating [19]. The measured value of η_s was 12.4%, and unknown parameters about the LC distribution across the room temperature fabricated grating were calculated as $c_{25\,^\circ C} = 0.176$, $f_{25\,^\circ C} = 0.239$. After the measurement for diffraction efficiency, the grating was cooled to room temperature and LC molecules in the pure LC layer relaxed to their original orientation along the grating vector. This is indicated by the recovery of the high diffraction efficiency for p-polarized light. The calculation of refractive index contrast for feedback lights is slightly different from the isotropic grating due to the alignment of LC molecules, $n_{\text{LC rich region}} = f n_o + (1 - f) n_{\text{polymer matrix}} = 1.532$, $n_{\text{polymer rich}} = n_{\text{polymer matrix}} = 1.5352$, $\Delta n = 0.0032$. Interestingly enough, the pure LC layer in a room temperature fabricated transmission grating serves as a low index region for feedback lights.

From the calculation we can see that about 25% more liquid crystal is phase separated out to form the pure liquid crystal layer at high fabricating temperature. This is because a good diffusion of monomers can be realized when the LC is in

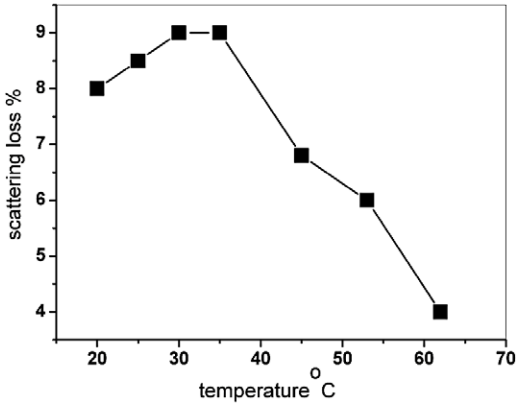

Figure 8. Scattering loss as a function of fabrication temperature.

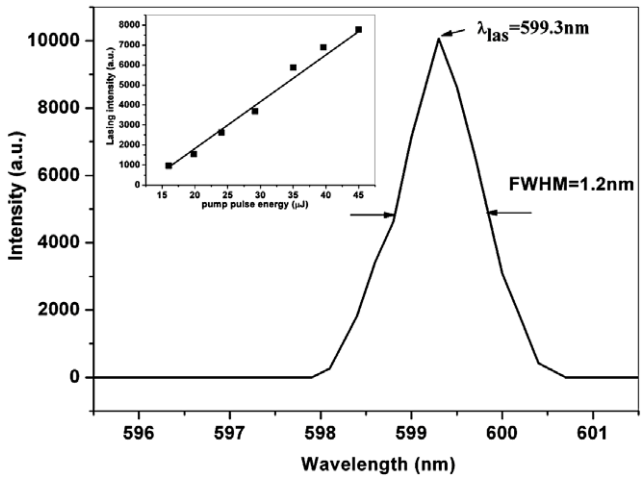

Figure 9. Lasing spectra of the DCM-doped room temperature fabricated transmission grating. The inset shows the corresponding output lasing intensity as a function of the pumping energy.

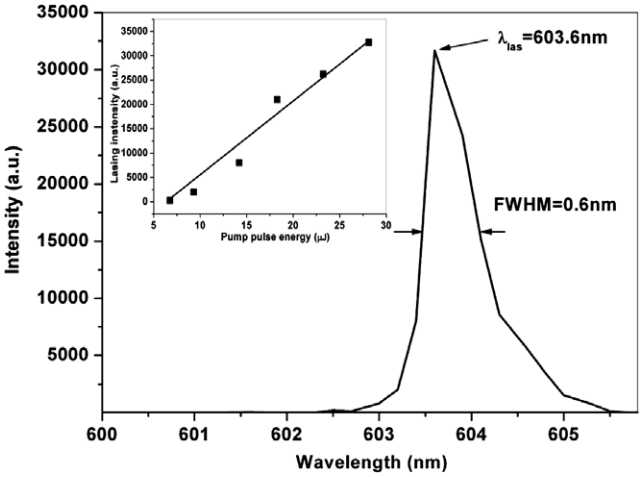

Figure 10. Lasing spectra of the DCM-doped high temperature fabricated transmission grating. The inset shows the corresponding output lasing intensity as a function of the pumping energy.

the isotropic state, and the high monomer diffusion coefficient guarantees a comparatively more thorough redistribution of monomers and LC before the gelatin of the polymer [20]. Also, the RI contrast for feedback lights can be increased from 0.0032 to a comparatively high value of 0.0144; selection of a suitable LC may further increase this value.

3.3. Decrease of scattering loss

When light impinges onto the transmission grating at the Bragg angle, higher-order ($\geqslant 2$) diffraction by the grating can be neglected. Light losses are due to glass reflections, material absorption, and grating scattering. Absorption loss of the dye is negligible in the long wavelength region (>600 nm) [9], thus grating scattering loss can be defined [21] as $\sigma = (I_{\text{in}} - I_0 - I_1 - I_{\text{re}})/I_{\text{in}}$. The dependence of grating scattering loss on fabricating temperature is shown in figure 8. It is clear that scattering loss decreases significantly from 8% to 4% by raising the fabricating temperature to the LC clearing point. According to Sutherland [22] scattering inside the HPDLC structure mainly comes from refractive index inhomogeneities in the high refractive index region, while the roughness of interface plays a comparatively minor role. RI variation inside the HPDLC gratings has two major sources, It may come from LC droplets with different average orientations, and it also may come from the LC–polymer matrix difference. As there is no evidence of LC droplet formation in our scaffolding-like HPDLC morphology, we think the larger volume fraction of phase separated LC in the high temperature fabricated grating decreases the LC–matrix RI variations and thus reduces the scattering loss inside the transmission grating.

3.4. Result of the lasing measurement

The lasing spectra of a DCM-doped room temperature fabricated transmission grating is shown in figure 9, the inset shows the output lasing intensity as a function of the pumping energy. The corresponding experimental results of a DCM-doped high temperature fabricated transmission grating are shown in figure 10. The lasing peaks are 599.3 nm and 603.6 nm respectively. As indicated by the equation of Kogelnik's coupled wave theory for a DFB laser [23]:

$$\lambda_{\text{las}} = \frac{2n_{\text{eff}}\Lambda}{m} \tag{5}$$

where Λ is the grating pitch (777 nm) and n_{eff} is the effective index of the grating estimated to be 1.55. m is the diffraction order of the grating, in this paper $m = 4$ and the calculated output lasing wavelength should be 602 nm, which falls in the fluorescence emission band of DCM [9]. The experimental results strictly agree with the calculation; the small difference in the lasing wavelengths of the two gratings can be attributed to the difference in the average RI of the grating due to different alignment of LC molecules. FWHM of the lasing is reduced from 1.2 to 0.6 nm, the narrowest value ever reported for doped 1D HPDLC gratings. The threshold of the lasing is reduced from 17 to 6 μJ/pulse, besides, the lasing intensity is

much stronger from a high temperature fabricated transmission grating than that from a room temperature fabricated grating under the same pumping energy, and this shows the energy conversion is also improved. These results are reasonable considering the arguments presented above, as the high temperature fabricated transmission offers a high refractive index contrast (0.0144 evinced by the above calculation) for decreasing the FWHM [24] and low scattering for lowering the threshold of the laser emission.

4. Conclusions

In this work, we investigated the effects of fabricating temperature on an HPDLC transmission grating, and found that the highly anisotropic grating fabricated at room temperature becomes polarization-independent by its clearing point. Also, a more complete phase separation of liquid crystal from polymer is demonstrated. Besides, optical measurement carried out at the Bragg angle shows a 50% scattering loss decrease. Although this high temperature fabricated grating shows a polarization-independent behavior at the expense of lower diffraction efficiency, we found it to be excellently suitable in DFB laser applications; the refractive index modulation can be as high as 0.0144 evidenced by the above calculation. The experimental result of this transmission grating as a distributed feedback laser shows a lasing output with a FWHM of about only 0.6 nm and a threshold of 6 μJ/pulse. Besides, the decreased scattering loss nature of this grating can improve the energy conversion efficiency and decrease the divergence angle of the HPDLC DFB laser. In this way we greatly improved the lasing properties in the 1D HPDLC structure.

Acknowledgments

The authors would like to thank the support from the Natural Science Foundation of China (grant Nos 60578035, 50473040, and 60736042).

References

[1] Sutherland R L, Natarajian L V, Tondiglia V P and Bunning T J 1993 *Chem. Mater.* **5** 1533–8
[2] Yablonovitch E 1987 *Phys. Rev. Lett.* **58** 2059–62
[3] Date M, Takeuchi Y and Kato K 1998 *J. Phys. D: Appl. Phys.* **31** 2225–30
[4] Li M S, Wu S T and Fuh A Y G 2006 *Appl. Phys. Lett.* **88** 091109
[5] De Sio L, Tabiryan N, Caputo R, Veltri A and Umeton C 2008 *Opt. Express* **16** 7619–24
[6] Lee J H, Lee S J, Song J B, Lee Y W and Kwak C H 2003 *Proc. SPIE* **5261** 237
[7] Jakubiak R, Bunning T J, Vaia R A, Natarajan L V and Tondiglia V P 2003 *Adv. Mater.* **15** 241–4
[8] Hsiao V K S, Lu C, He G S, Pan M, Cartwright A N, Prasad P N, Jakubiak R, Vaia R A and Bunning T J 2005 *Opt. Express* **13** 3787–94
[9] Liu Y J, Sun X W, Shum P, Li H P, Mi J, Ji W and Zhang X H 2006 *Appl. Phys. Lett.* **88** 061107
[10] Jakubiak R, Tondiglia V P, Natarajan L V, Sutherland R L, Lloyd P, Bunning T J and Vaia R A 2005 *Adv. Mater.* **17** 2807–11
[11] Vardanyan K K, Qi J, Eakon J N, De Sarkar M and Crawford G P 2002 *Appl. Phys. Lett.* **81** 4736–8
[12] Butler J J, Malcuit M S and Rodriguez M A 2002 *J. Opt. Soc. Am.* B **19** 183–9
[13] Caputo R, De Sio L, Veltri A, Umeton C and Sukhov A V 2004 *Opt. Lett.* **29** 1261–3
[14] Sutherland R L, Natarajan L V, Tomdiglia V P, Chandra S, Shepherd C K, Brandelik D M and Siwecki S A 2002 *J. Opt. Soc. Am.* B **19** 3004–12
[15] Natarajan L V, Shepherd C K, Brandelik D M, Sutherland R L, Chandra S, Tondiglia V P, Tomlin D and Bunning T J 2003 *Chem. Mater.* **15** 2477–84
[16] Fan Y-H *et al* 2004 *Appl. Phys. Lett.* **84** 1233–5
[17] Holmes M E and Malcuit M S 2002 *Phys. Rev.* E **65** 066603
[18] Kogelnik H 1969 *Bell Syst. Tech. J.* **48** 2909
[19] Caputo R, Veltri A, Umeton C and Sukhov A V 2005 *J. Opt. Soc. Am.* B **22** 735–42
[20] Caputo R, Sukhov A V, Tabirian N V, Umeton C and Ushakov R F 2001 *Chem. Phys.* **271** 323–35
[21] Vita F, Lucchetta D E, Castagna R, Criante L and Simoni F 2009 *J. Opt. A: Pure Appl. Opt.* **11** 024021
[22] Sutherland R L, Tondiglia V P, Natarajan L V, Lloyd P F and Bunning T J 2006 *J. Appl. Phys.* **99** 123104
[23] Kogelnik H and Shank C V 1971 *J. Appl. Phys.* **43** 2327–35
[24] Kogelnik H and Shank C V 1971 *Appl. Phys. Lett.* **18** 152–4